5

CENTRAL RESEARCH LIBRARY
DOCUMENT COLLECTION

MARTIN MARIETTA ENERGY SYSTEMS LIBRARIES
3 4456 0351041 2

ORNL-2672
Metallurgy and Ceramics

Cy 5

EDDY-CURRENT MEASUREMENT OF METAL THICKNESS AND CLADDING THICKNESS

R. A. Nance
J. W. Allen

CENTRAL RESEARCH LIBRARY
DOCUMENT COLLECTION
LIBRARY LOAN COPY
DO NOT TRANSFER TO ANOTHER PERSON
If you wish someone else to see this document, send in name with document and the library will arrange a loan.

OAK RIDGE NATIONAL LABORATORY
operated by
UNION CARBIDE CORPORATION
for the
U.S. ATOMIC ENERGY COMMISSION

LEGAL NOTICE

This report was prepared as an account of Government sponsored work. Neither the United States, nor the Commission, nor any person acting on behalf of the Commission:

A. Makes any warranty or representation, express or implied, with respect to the accuracy, completeness, or usefulness of the information contained in this report, or that the use of any information, apparatus, method, or process disclosed in this report may not infringe privately owned rights; or

B. Assumes any liabilities with respect to the use of, or for damages resulting from the use of any information, apparatus, method, or process disclosed in this report.

As used in the above, "person acting on behalf of the Commission" includes any employee or contractor of the Commission to the extent that such employee or contractor prepares, handles or distributes, or provides access to, any information pursuant to his employment or contract with the Commission.

ORNL-2672

Contract No. W-7405-eng-26

METALLURGY DIVISION

EDDY-CURRENT MEASUREMENT OF METAL THICKNESS AND CLADDING THICKNESS

R. A. Nance
J. W. Allen

DATE ISSUED

MAR 31 1959

OAK RIDGE NATIONAL LABORATORY
Oak Ridge, Tennessee
Operated by
UNION CARBIDE CORPORATION
for the
U.S. ATOMIC ENERGY COMMISSION

MARTIN MARIETTA ENERGY SYSTEMS LIBRARIES

3 4456 0351041 2

EDDY-CURRENT MEASUREMENT OF METAL THICKNESS AND CLADDING THICKNESS

R. A. Nance and J. W. Allen

ABSTRACT

The basic principles of eddy-current testing as applied to metal thickness and cladding-thickness measurements are discussed. The results of a series of studies are illustrated with graphs of the impedance of an eddy-current probe coil as a function of the various test parameters, including frequency, conductivity, thickness, and "lift-off" or distance between the probe and metal surface. A special phase-measuring technique is described whereby it is possible to completely eliminate lift-off signals while measuring the thickness of nonferromagnetic claddings on ferromagnetic bases. The potential of this technique for automatic, high-speed gauging is discussed. Results are presented illustrating the capability of eddy-current methods to accurately and reliably measure cladding thickness.

INTRODUCTION

The field of nuclear energy along with other technical fields continues to demand increasing strength and corrosion-resistance characteristics of metals and alloys. Since, in many instances, no one material can meet all of the metallurgical requirements demanded of a part, or assembly, many duplex and clad assemblies are used which allow maximum utilization of the desired characteristics of the individual materials. To ensure the integrity of such an assembly, a nondestructive testing method is necessary which can accurately measure the thickness of the different plies in the assembly.

The Nondestructive Test Development Group, Metallurgy Division, Oak Ridge National Laboratory, has conducted an investigation of eddy-current inspection as applied to metal-thickness and cladding-thickness measurements and developed techniques to perform these measurements. The purpose of this paper is to present the theory of this method, the techniques which are employed, and some results which illustrate its use.

A brief study of the principles of induced eddy currents will be of value in understanding their application to the problem of cladding-thickness measurements.

EDDY-CURRENT TESTING

In essence, the method consists of inducing eddy currents into the metal part to be inspected by bringing it into the electromagnetic field of a coil which is being supplied with an alternating current. The original field of the coil is altered according to the amplitude, phase, and distribution of the induced eddy currents. This change in the original field is utilized to describe the characteristics of the specimen under surveillance.

In general, the alteration of the field produced by the eddy currents is a function of the frequency of the exciting current, the characteristics of the original field, the electrical conductivity and magnetic permeability of the part, its physical dimensions and location in the field, and the presence of discontinuities or "inhomogeneities" within the part. Since the mechanical and thermal history of the part influence its electrical conductivity (and its magnetic permeability in the case of austenitic stainless steels), they also become influencing factors.

The type of coil selected for this investigation was a surface probe coil contained in a small cup-shaped high-permeability core and having its axis perpendicular to the surface of the part. This type coil was selected since it can be used to examine most surface configurations, it is relatively easy to fabricate, and its inherent sensitivity is high because of the high-permeability core. Because of the large number of variables encountered in using this type of coil, no theory which comprehensively describes the alteration of its field has been formulated; therefore, logical predictions can be made only after much experimentation.

The changes in the field of the testing coil just described take place in both amplitude and phase and are directly related to the impedance of the coil. This impedance can be measured by driving the coil with a constant amplitude current and measuring the amplitude and phase changes of the voltage across the terminals of the coil. A plot of the amplitude and phase variations in the impedance of a theoretical probe coil are

shown in Fig. 1 (ORNL-LR-DWG 30635). This plot has been converted from the polar co-ordinates of amplitude and phase measurements to rectangular co-ordinates for discussion purposes. The reactive axis of this plot can be associated with the energy stored in the system during each cycle of the alternating current flowing through the coil; the resistive axis can be associated with the energy dissipated in the system during each cycle. When the coil is surrounded by air, which has an electrical conductivity of zero, no eddy currents will be induced. Therefore, the impedance of the coil will be determined by the reactance and resistance of the coil. For purposes of discussion, the impedance values are normalized to the reactance of the coil in air.

If an apparent infinitely thick nonferromagnetic specimen* having a conductivity slightly greater than zero is placed in the field of the coil, eddy currents will be induced in it and will affect the impedance of the test coil in two ways: the induced eddy currents will create their own electromagnetic field which will oppose the field of the coil, resulting in a decrease of the energy stored in the system; and at the same time, the flow of eddy currents through the finite resistance of the part will dissipate energy in the form of heat. Continual increase of either the conductivity or the frequency of the alternating current in the coil will cause the reactive component to continually decrease, while the resistive component is first caused to increase to a maximum and then decrease. This can be illustrated on Fig. 1 by the three points a, b, and c. Assuming a relative permeability (μ_r) of one and a current of constant frequency, these three points represent the impedance of the coil in the presence of three metals whose conductivities are different according to the relationship $\gamma_a < \gamma_b < \gamma_c$. If the conductivity is held constant and μ_r remains one, these three points represent the impedance caused by different coil current frequencies according to the relationship $f_a < f_b < f_c$.

An increase in μ_r tends to enlarge the curve generated by γ and f, as illustrated in Fig. 1 by the line connecting points b, b', and b". If f and γ are constant, b, b', and b" represent the impedance of the coil in

*Thicker than the effective depth of penetration of the eddy currents which is a function of γ, f, μ_r, and the size and shape of the field of of the coil.

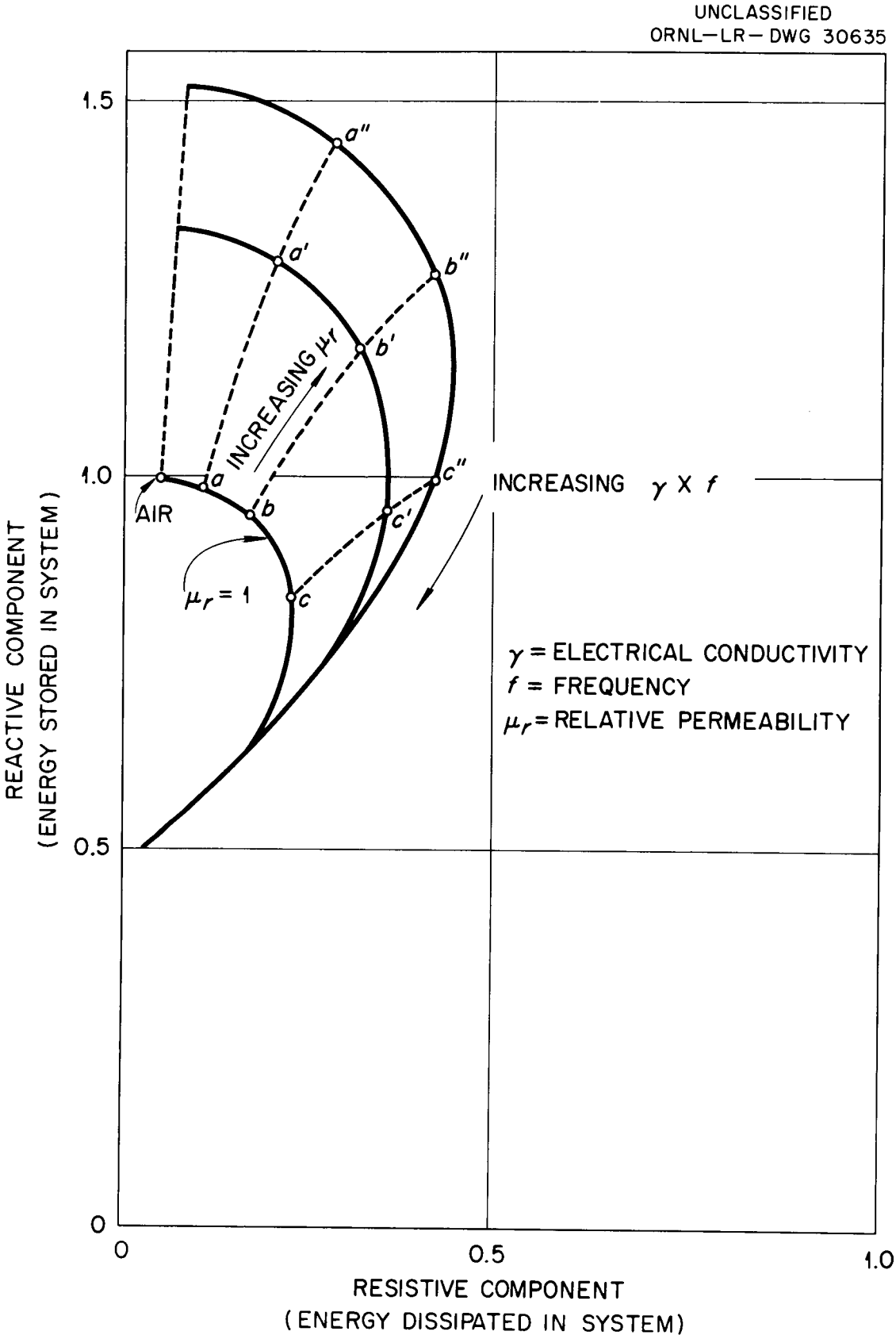

Fig. 1. Normalized Probe Coil Impedance Variations.

the presence of three specimens having the same conductivity but different permeabilities according to the relationship $\mu_{rb} < \mu_{rb'} < \mu_{rb''}$.

A plot of the actual impedance variations of a probe coil produced at 20 kc by varying conductivity (γ) when $\mu_r = 1$ is shown in Fig. 2 (ORNL-LR-DWG 19103A). For simplicity of discussion, the initial resistive component is ignored and the coil assumed to be a perfect inductor having only a reactive impedance when surrounded by air. Figure 3 (ORNL-LR-DWG 19104A) is a plot of the impedance variations of the same probe coil as a function of frequency with $\mu_r = 1$ and with $\gamma = 45\%$ IACS (International Annealed Copper Standard).

THICKNESS MEASUREMENTS

Eddy-current thickness measurements utilize the impedance variations produced in a probe coil when the thickness of the specimen is allowed to become less than an apparent "infinite" thickness. Figure 4 (ORNL-LR-DWG 19105R) is a plot of the impedance variations of the coil at 20 kc for varying thicknesses of 6061-aluminum alloy in the presence of the coil. It should be noted that the curve generated by increasing thicknesses of aluminum is very similar in shape to the γ x f curve of Fig. 1. Also shown is the effect on the impedance of the coil by lift-off or the distance between the probe and the specimen under examination. The lift-off curve has the same characteristic shape, regardless of the thickness of the specimen, being complex in shape and having at least two inflection points. In the experience of the authors, the complex shape of these curves is not particular to any given coil; however, the degree of complexity has been observed to vary. The reason for this phenomenon is not understood.

In all of the data presented thus far, it has been assumed that the coil is a perfect inductor having no resistance. However, this is not true in practice, as illustrated in Fig. 5 (ORNL-LR-DWG 26996R), which shows the true impedance variations of a probe coil as a function of 1100-aluminum thickness. It should be noted that the resistive component of the coil's impedance is almost as large as the reactive component. However, this will vary depending upon the coil parameters.

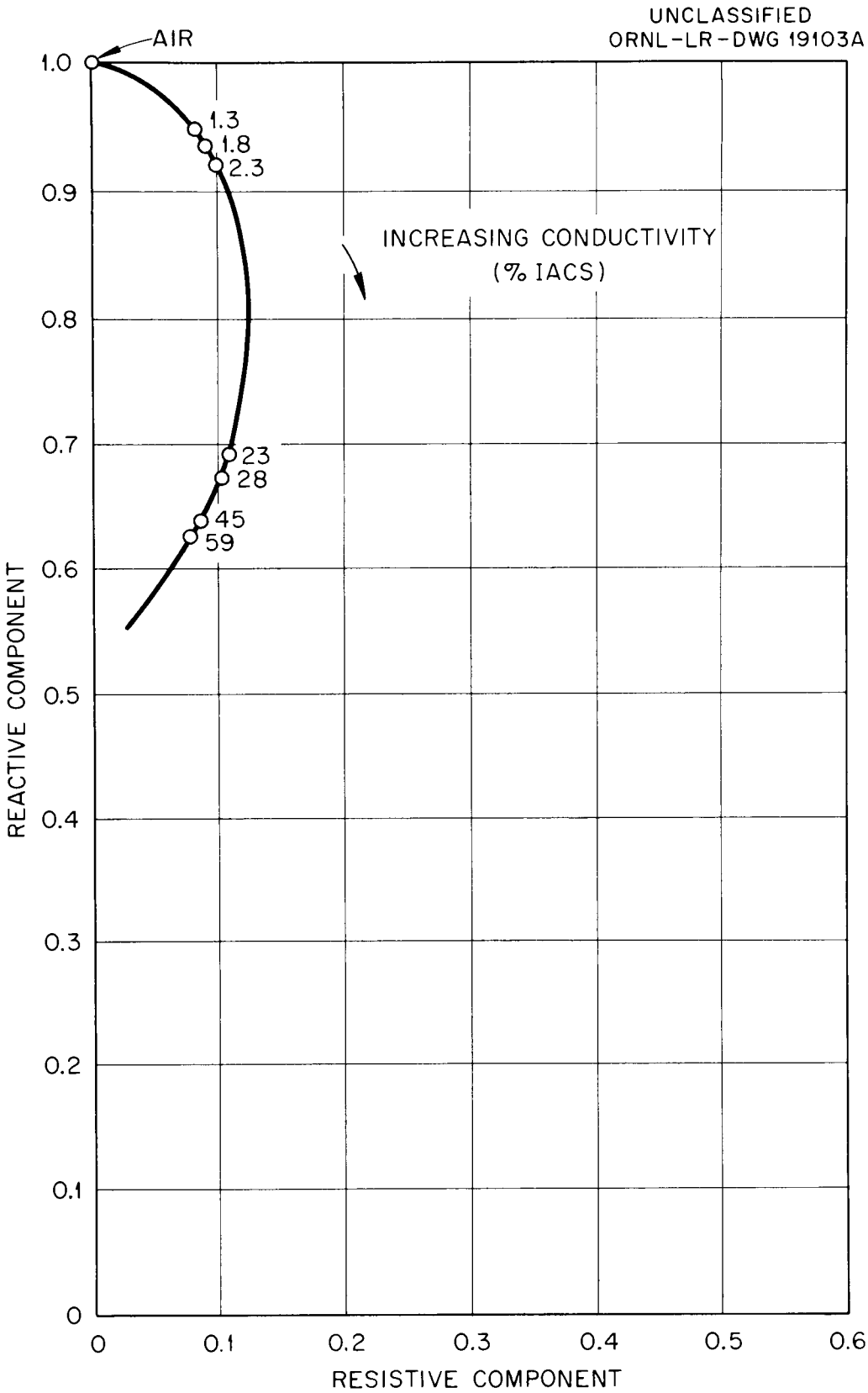

Fig. 2. Normalized Impedance Plot of Mark X Probe Coil as a Function of Varying Conductivity at 20 kc.

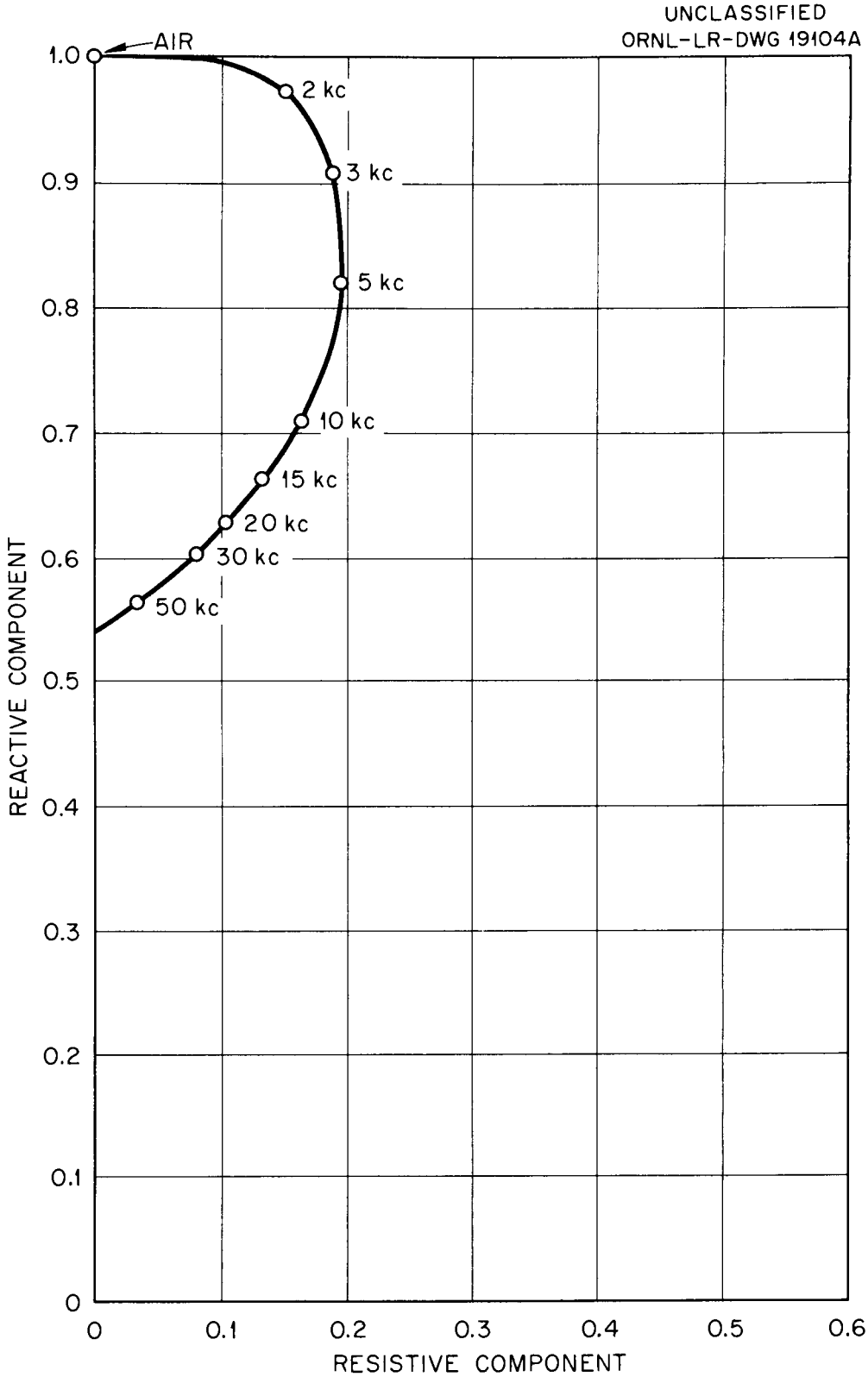

Fig. 3. Normalized Impedance Plot of Mark X Probe Coil as a Function of Varying Frequency in Presence of 6061 Aluminum Alloy (γ = 45% IACS).

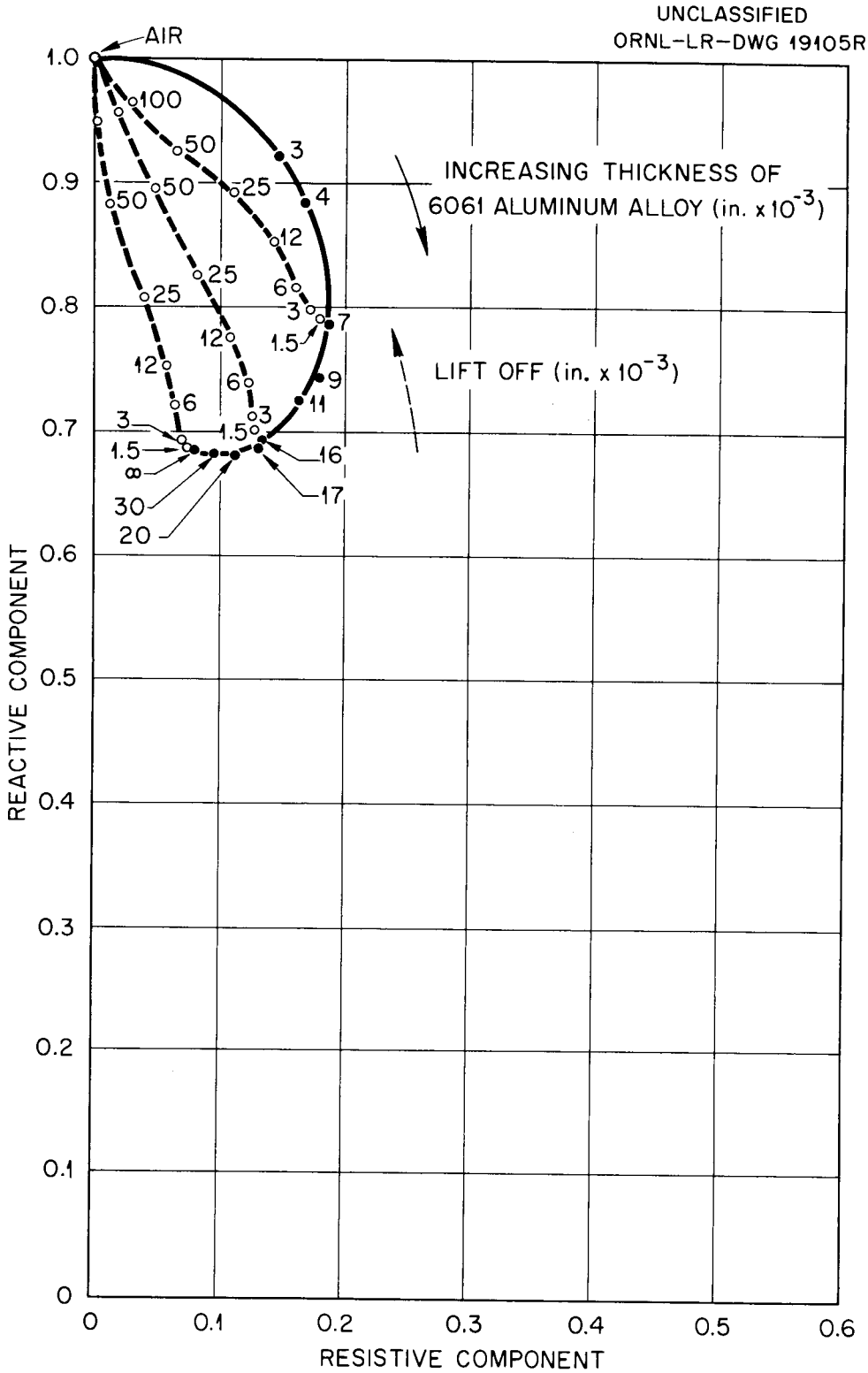

Fig. 4. Normalized Impedance Plot of Mark X Probe Coil in Presence of Varying Thickness of 6061 Aluminum Alloy (Conductivity = 45% IACS) at 20 kc with Lift-Off Effect Shown.

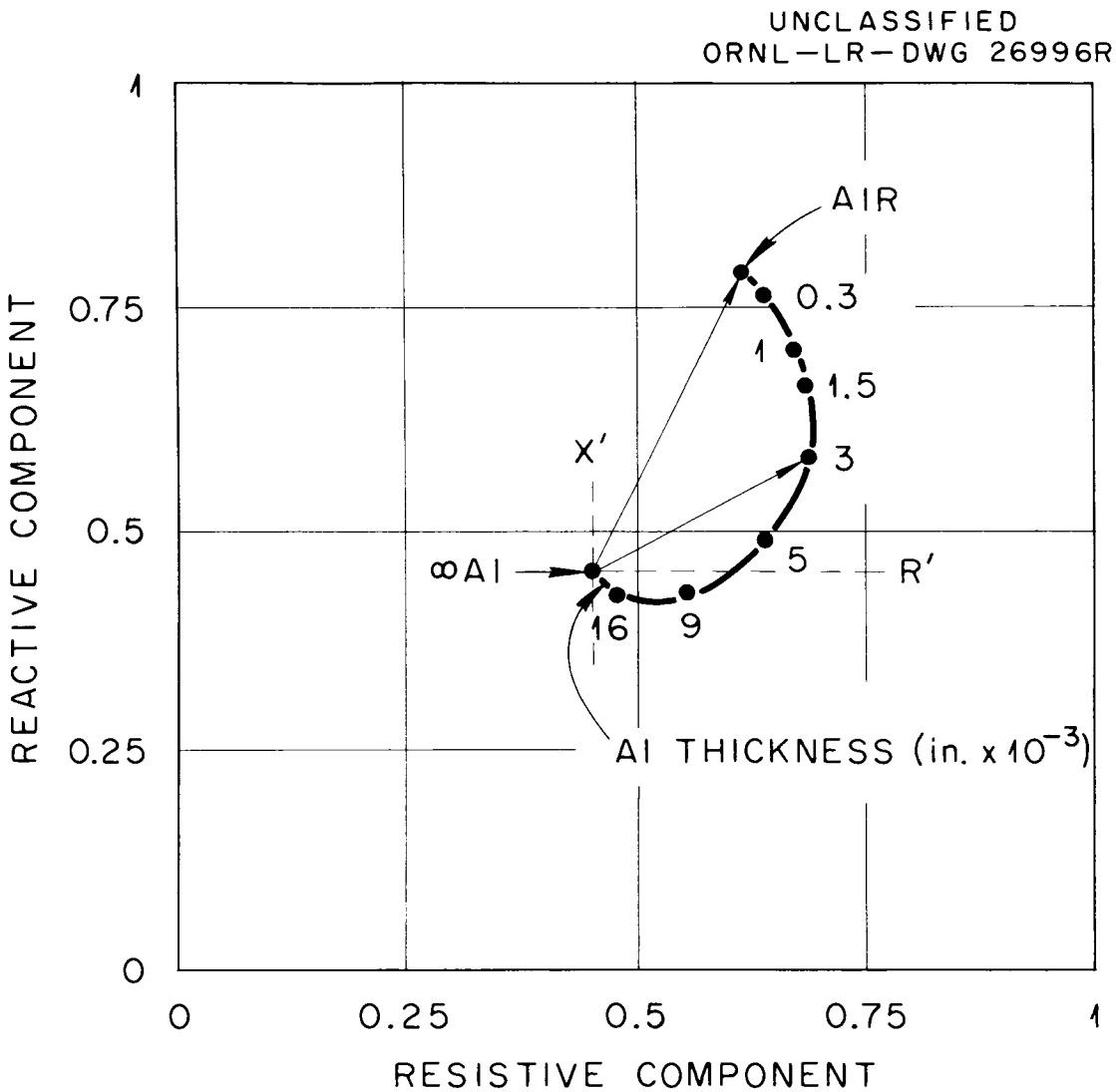

Fig. 5. Normalized Probe Coil Impedance Variation for Varying Thicknesses of Aluminum in Air at 20 kc.

The impedance variations produced by changes in thickness of a specimen under examination are often relatively small compared to the absolute value of the impedance of the coil. Since the absolute impedance is of little value and since small impedance changes are difficult to measure, a technique was employed by which these changes could be measured accurately. Using electronic subtracting circuitry, it is possible to shift the origin to a new point indicated by the X' and R' axes on Fig. 5 and to measure impedance changes with respect to the new origin.

Each point on the impedance curve can be represented by an impedance vector drawn to that point from the new origin, and in addition, each vector has a unique length and phase angle with respect to the axes. A measurement of either the amplitude or phase angle of an impedance vector can be correlated with the metal thickness in the field of the probe. Since both are unique, only one is necessary to describe the specimen thickness.

The use of impedance-amplitude measurements for making thickness measurements is illustrated in Fig. 6 (ORNL-LR-DWG 23879). This is a plot of relative vector amplitude, as read on a meter, against the thickness of the aluminum specimen. A similar plot can be made to correlate phase-angle variations with thickness changes.

In the use of these techniques, it is necessary to eliminate the undesirable effects due to lift-off variations which adversely affect the accuracy of measurement. For making measurements on flat surfaces this can most easily be accomplished by mechanical methods, whereas in other applications this problem may be solved more readily by special electronic circuitry.

CLADDING-THICKNESS MEASUREMENTS

Cladding-thickness measurements utilize the impedance variations caused by the presence of two metals in the field of the probe coil. An example of this is illustrated in Fig. 7 (ORNL-LR-DWG 19108R), in which the impedance changes produced at 20 kc both by varying thicknesses of copper on a thick base of Inconel and by varying thicknesses of Inconel on a thick base of copper are plotted.* It should be emphasized

*The initial resistive component of the coil is neglected.

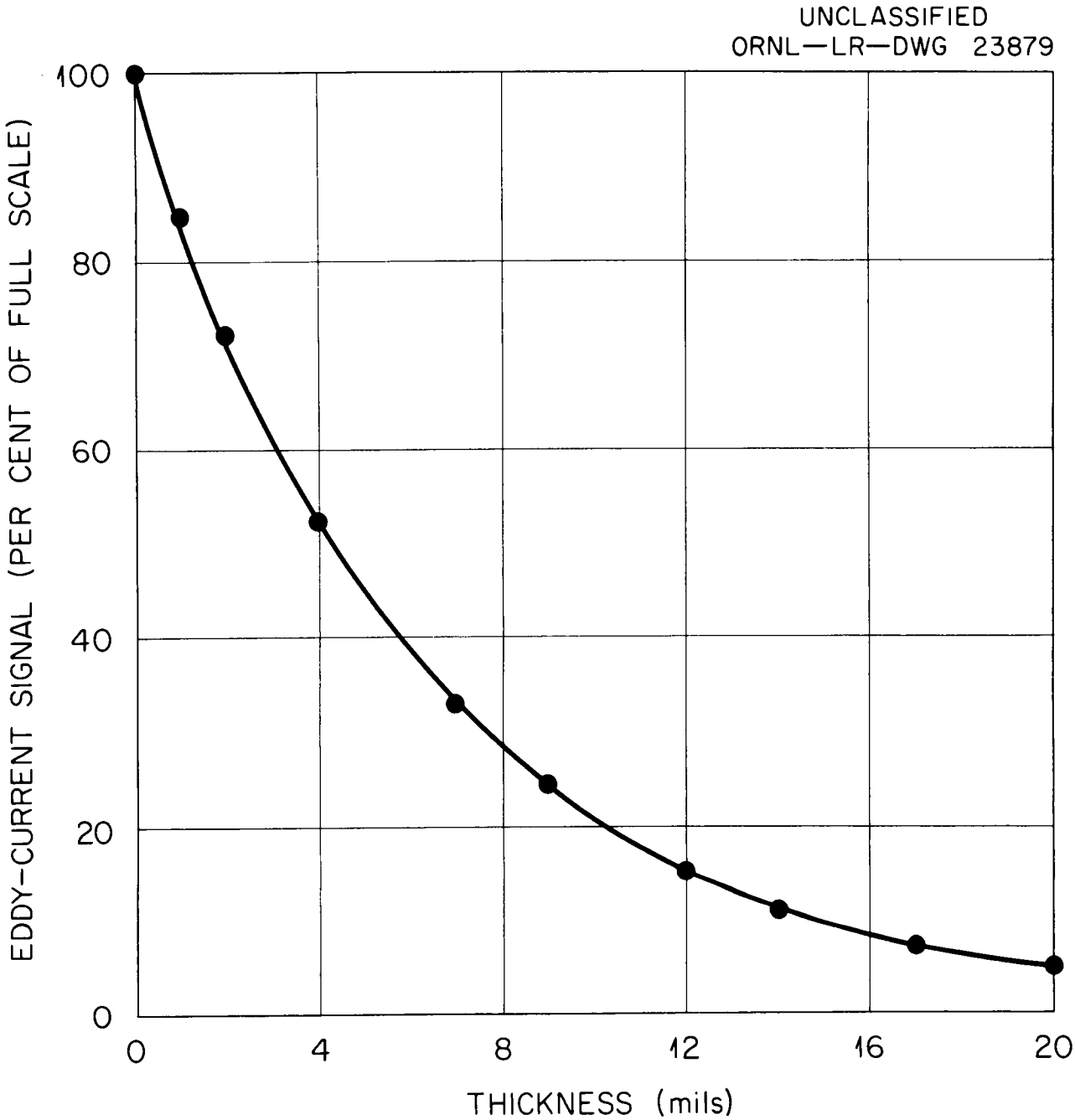

Fig. 6. Eddy-Current Thickness Gage Calibration Curve for 1100 Aluminum (Conductivity: 59% IACS).

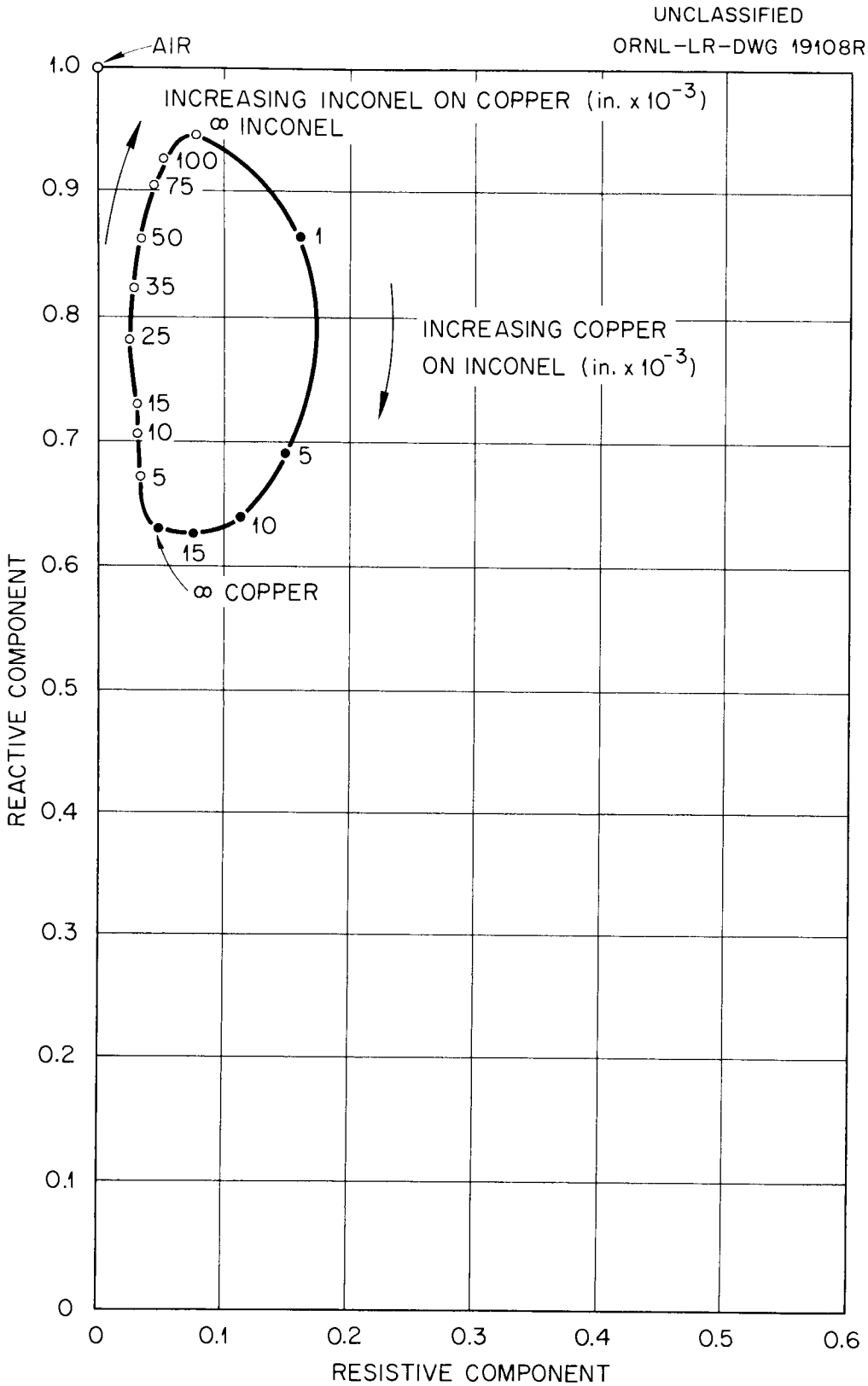

Fig. 7. Normalized Impedance Plot of Mark X Probe Coil in Presence of Copper (Conductivity = 85% IACS) and Inconel (Conductivity = 1.8% IACS) at 20 kc.

that laminations in the specimen do not noticeably affect the eddy-current flow which is horizontal to the surface, while a surface crack perpendicular to the surface does adversely affect the eddy-current flow and introduce errors. These factors allow the use of standards built up from shims, having no metallurgical bond, to simulate bonded assemblies.

Note the similarity between the portion of the curve produced by copper on Inconel and the previous curves determined by varying the thickness of a single metal in the field of the coil. In contrast, the curve for Inconel on copper has a shape similar to lift-off curves. From these results it is concluded that there are two types of cladding-thickness measurements: the first is similar to a simple thickness measurement in which the cladding is the better conductor of the two materials involved and the second is similar to lift-off measurements in which the cladding is composed of the poorer conductor of the two. Of importance is the effect of conductivity on the apparent infinite thickness of the two metals. At a frequency of 20 kc, 0.030 in. of copper (γ = 85% IACS) appears infinitely thick to the eddy currents, while 0.130 in. of Inconel (γ = 1.8% IACS) are required to produce a similar effect.

The impedance curve for 6061-aluminum alloy cladding on a 48 wt % uranium-aluminum alloy at 20 kc is shown in Fig. 8 (ORNL-LR-DWG 19110). These are the materials used in a Materials-Test-Reactor-type fuel plate. An operating frequency of 20 kc was chosen as the optimum frequency for this investigation, since it allowed sufficient depth of eddy-current penetration to provide a measurement of the 0.020-in. nominal cladding thickness without penetrating through the 0.020-in. nominal core thickness. This prevented the cladding thickness variations on the "backside" of the plate from influencing the accuracy of measurement on the "frontside." Since the difference in the conductivities of the two materials is relatively small and the resulting impedance changes due to cladding thickness also are small, to measure these small impedance changes the axes were again shifted and the impedance changes amplified as illustrated in Fig. 9 (ORNL-LR-DWG 19107R). Each point on the cladding thickness curve again can be represented by a vector having a unique length and phase angle. A calibration curve similar to that shown in Fig. 6 was plotted to correlate cladding thickness with the impedance amplitude.

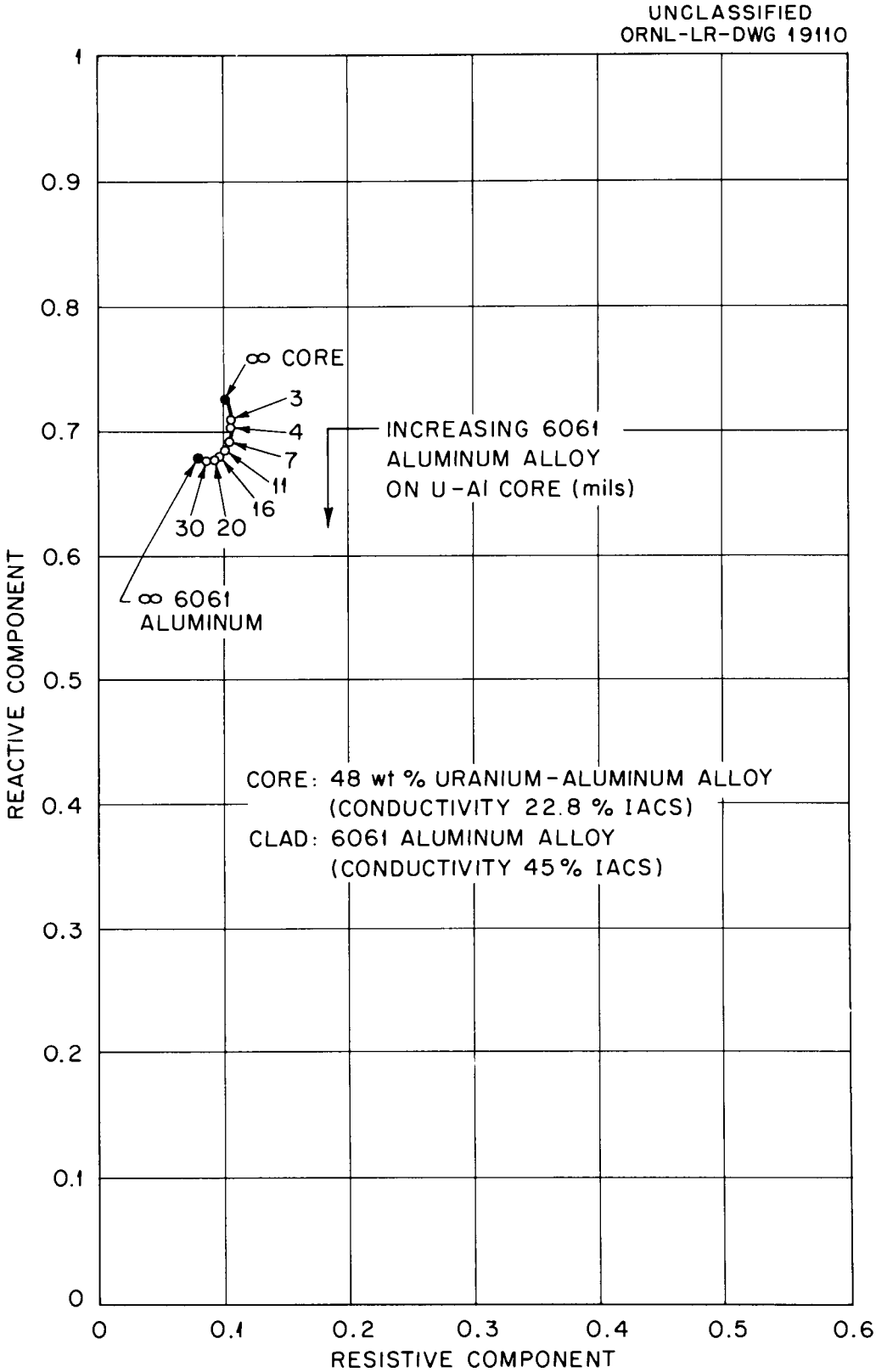

Fig. 8. Impedance Plane of Mark X Probe Coil in Presence of Mark X MTR Fuel Plate at 20 kc.

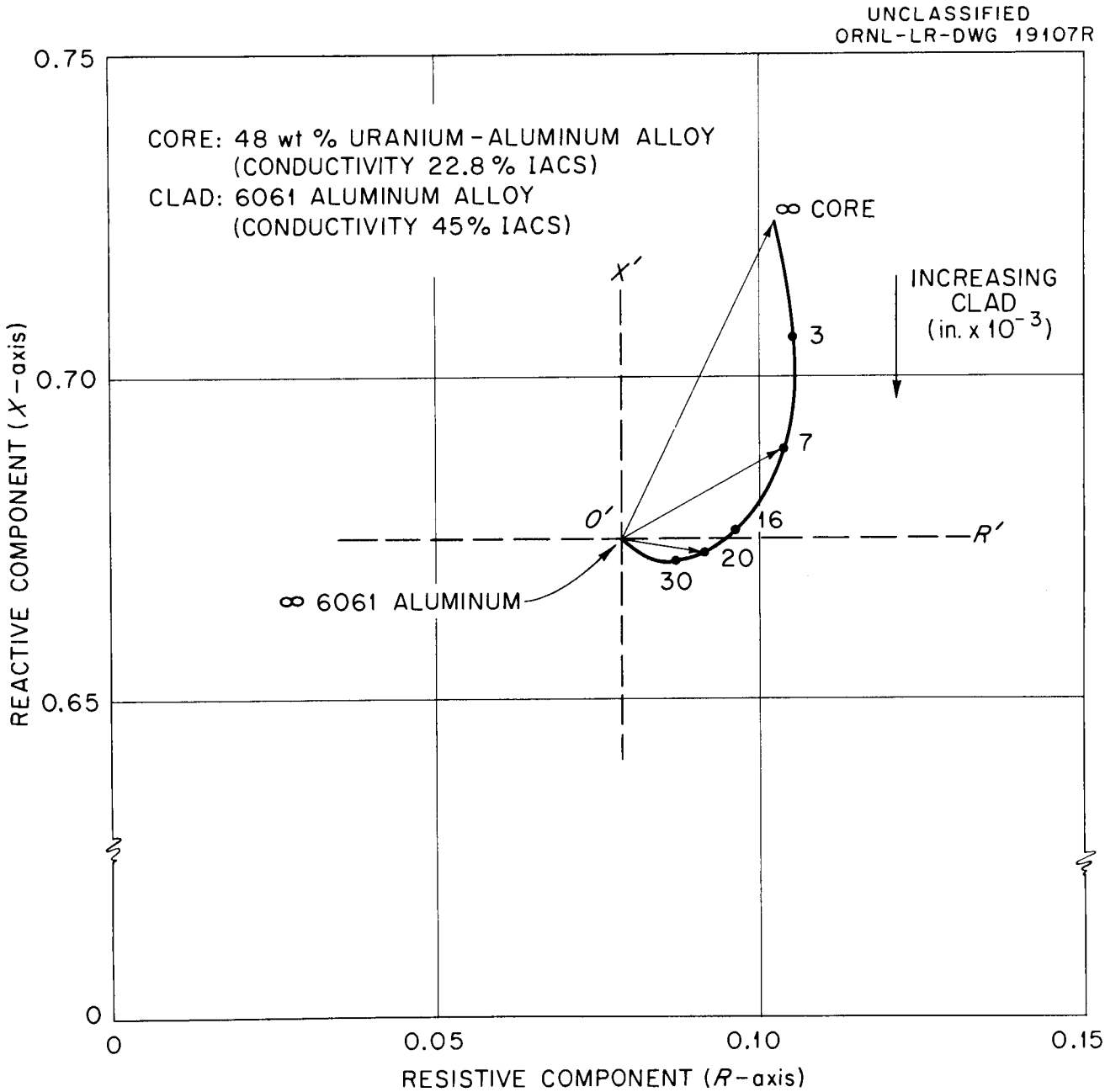

Fig. 9. Enlarged View of Normalized Impedance Plot of Mark X Probe Coil in Presence of Mark X MTR Fuel Plate at 20 kc.

This technique has been used successfully to measure the cladding on some MTR-type fuel plates to within 0.002 in. However, the accuracy of this technique is a function of the roughness of the interface between the two materials. As in metal-thickness measurements, the introduction of lift-off variations may introduce errors in measurement.

In the measurements described thus far, the impedance amplitude provided the most advantageous method of measurement. However, in the measurement of a nonmagnetic cladding on a ferromagnetic base, the phase-angle measuring techniques can be used most advantageously since it practically eliminates inaccuracies arising from lift-off variations.

The impedance variations produced by varying thicknesses of 1100 aluminum placed on a low carbon steel base are illustrated in Fig. 10 (ORNL-LR-DWG 26995). These are the same aluminum shims used to plot Fig. 5. The introduction of the ferromagnetic material tends to enlarge the curve of Fig. 5 and shift the upper end point to the impedance value of the coil on a thick specimen of steel. In order to measure the thickness of aluminum on the steel, the axes were shifted to the impedance value of the coil in air, as illustrated in Fig. 11 (ORNL-LR-DWG 26994R). As in previous cases, the points on the impedance curve can be represented by a unique vector length and phase angle.

The effect of lift-off also is shown in this plot. As lift-off is introduced between the specimen and the probe, the impedance changes are such that the amplitude of the impedance vector decreases while the phase angle remains constant. Therefore, if the phase angle is used as a measure of the cladding thickness, no error will be introduced by slight variations in the lift-off. Although it is not shown in this figure, a lift-off of 0.100 in. has been accommodated with this technique without adversely affecting the accuracy of measurement. Figure 12 (ORNL-LR-DWG 26997) is a calibration curve used to correlate these phase-angle changes with thickness variations.

The use of this technique in inspections requiring automatic scanning is greatly enhanced by the following: (1) the accuracy of measure is relatively independent of lift-off variations, and (2) intimate contact is not required between the probe and the specimen. For example, the high-speed measurement of thin nonferromagnetic foils can easily be accomplished

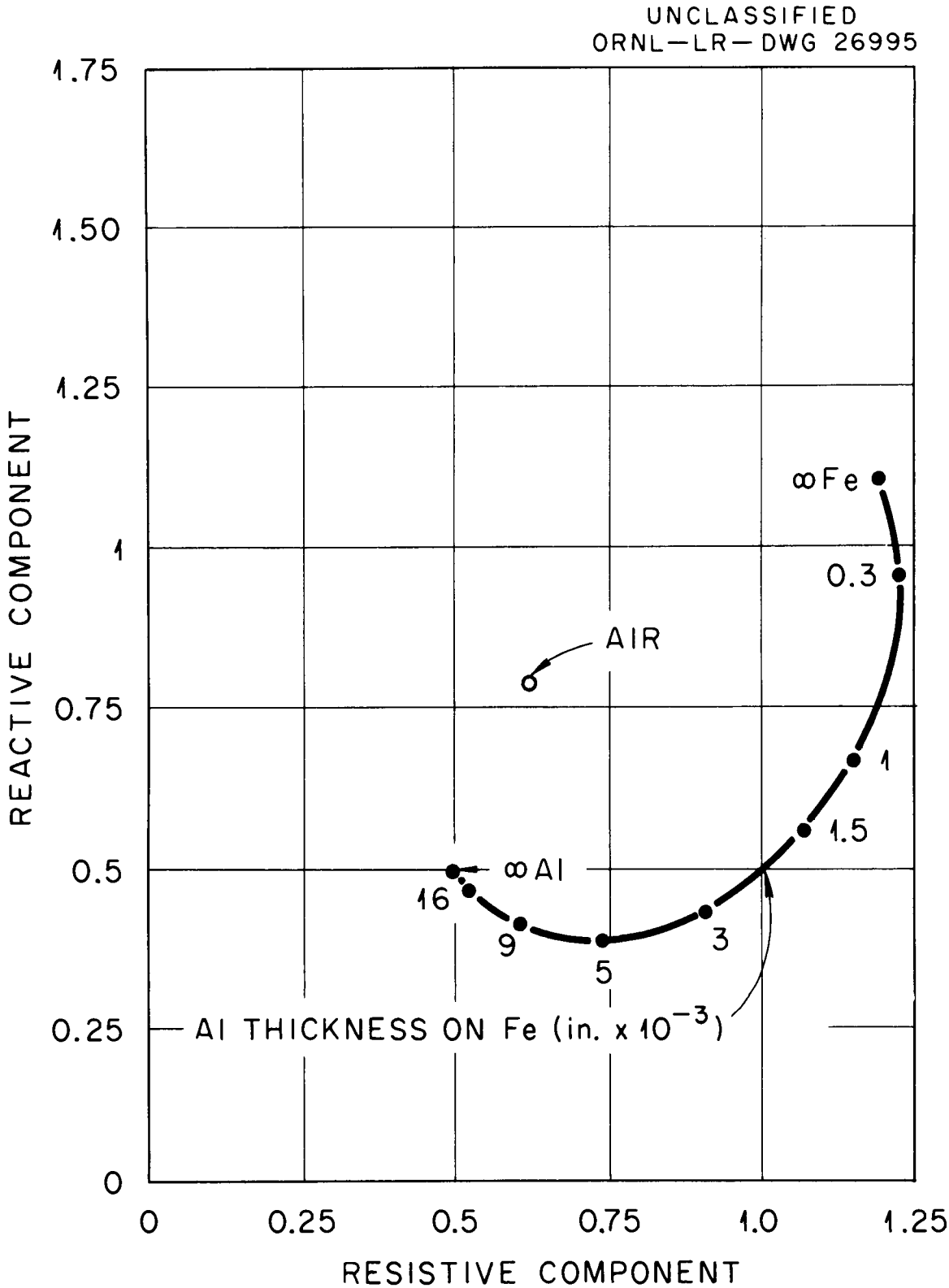

Fig. 10. Normalized Probe Coil Impedance Variations for Varying Thicknesses of Aluminum on Low Carbon Steel at 20 kc.

UNCLASSIFIED
ORNL—LR—DWG 26994R

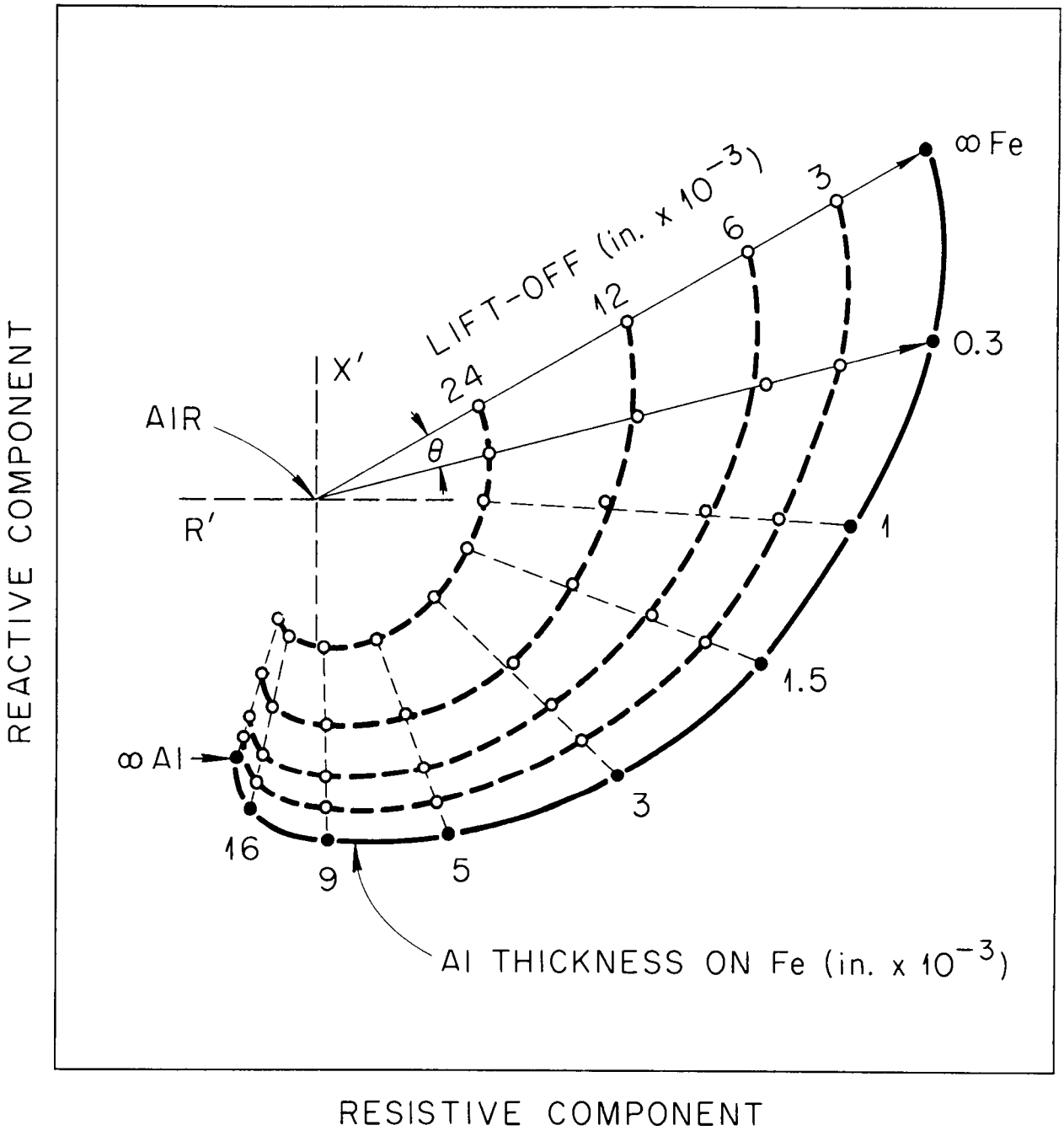

Fig. 11. Normalized Probe Coil Impedance Variations for Varying Thicknesses of Aluminum on Low Carbon Steel at 20 kc Referenced to Impedance of Probe Coil in Air.

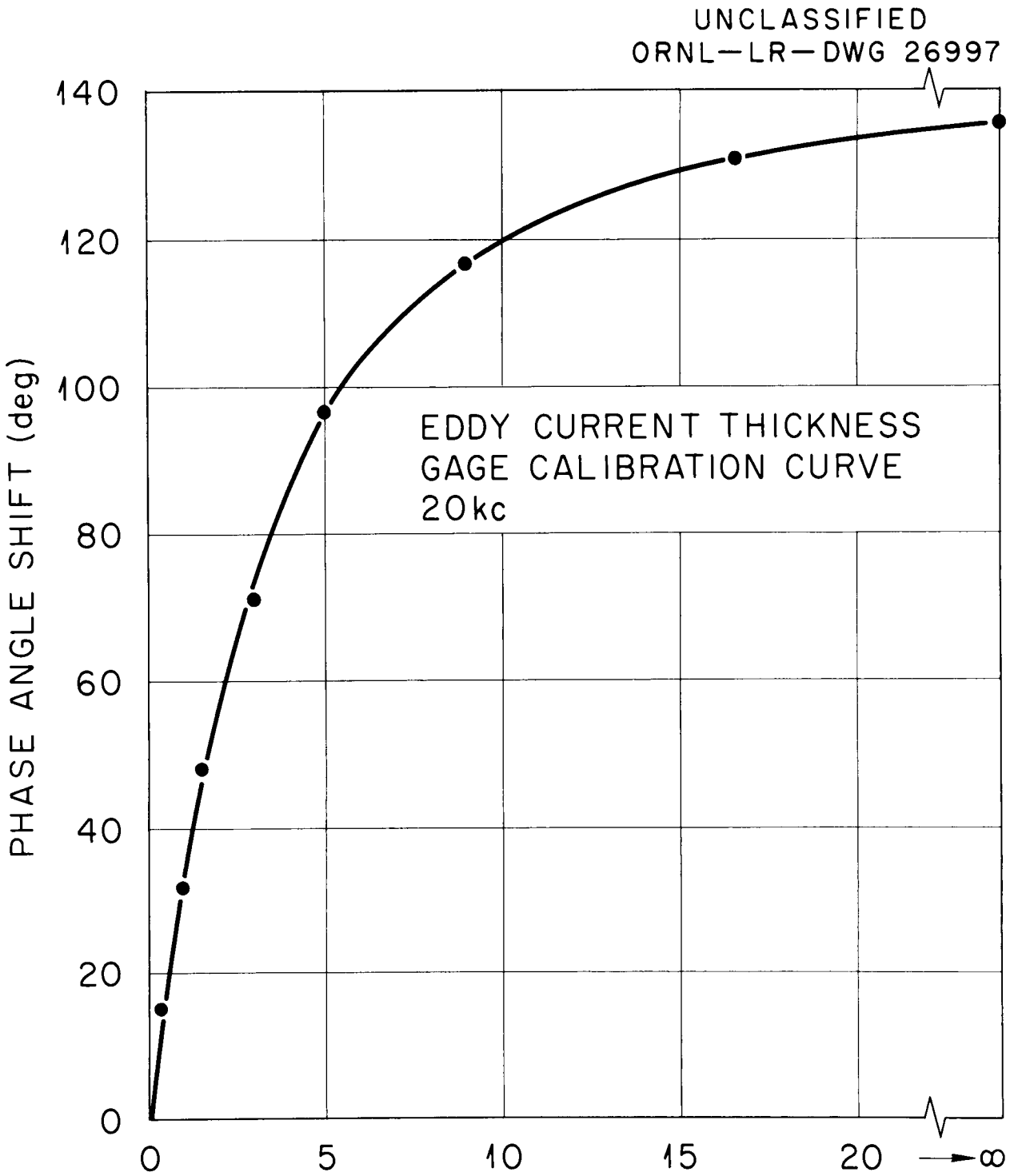

Fig. 12. Thickness of Aluminum on Low Carbon Steel (in. x 10^{-3}).

during the rolling operation if the foil is measured while passing over a ferromagnetic roller, since variation in lift-off due to vibrations of the machinery would not adversely affect the accuracy of measurement.

PROBE-COIL DESIGN

Since the depth of penetration of eddy currents into a part is important in thickness measurements, it is necessary to consider coil-design parameters controlling the size and shape of the field of the coil as these affect the depth of eddy-current penetration. Also, in determining the optimum test conditions, it is necessary to determine the relative sensitivity of different coil designs.

Two impedance curves as function of thickness are shown in Fig. 13 (ORNL-LR-DWG 19285R). These curves illustrate the advantage of using coils having high-permeability, low-loss cores. These curves were determined using two coils with identical windings, the one having a high-permeability core and the other having an air core. It is evident from the graph that all of the impedance changes are greatly increased by the high-permeability core; therefore, the intrinsic sensitivity of a probe-coil test is increased by the use of such cores. There are apparently no disadvantages to the use of these cores other than the slight fabrication problems imposed.

The depth of eddy-current penetration as a function of coil design is illustrated in Fig. 14 (ORNL-LR-DWG 33563). The solid lines show the response of two probe coils to thickness variations in type 304 stainless steel shims. Probe 1 is a solenoid-type coil consisting of 350 turns of No. 38 enameled copper wire wound on a 1/2-in. length of ferrite antenna rod. Probe 2 is a flat coil consisting of 200 turns of No. 42 enameled copper wire placed in a 3/16-in.-dia ferrite cup core. It is apparent that the depth of penetration of the eddy currents is much greater for Probe 1 than for Probe 2 as it is sensitive to thickness variations up to 0.200 in. while Probe 2 is only sensitive to thickness variations up to a total thickness of 0.140 in.

In theoretical treatment of eddy-current flow, the standard depth of eddy-current penetration has been defined as that depth at which the magnitude of the eddy currents has attenuated to e^{-1} or 36% of the value at the surface. Mathematically, this is expressed as

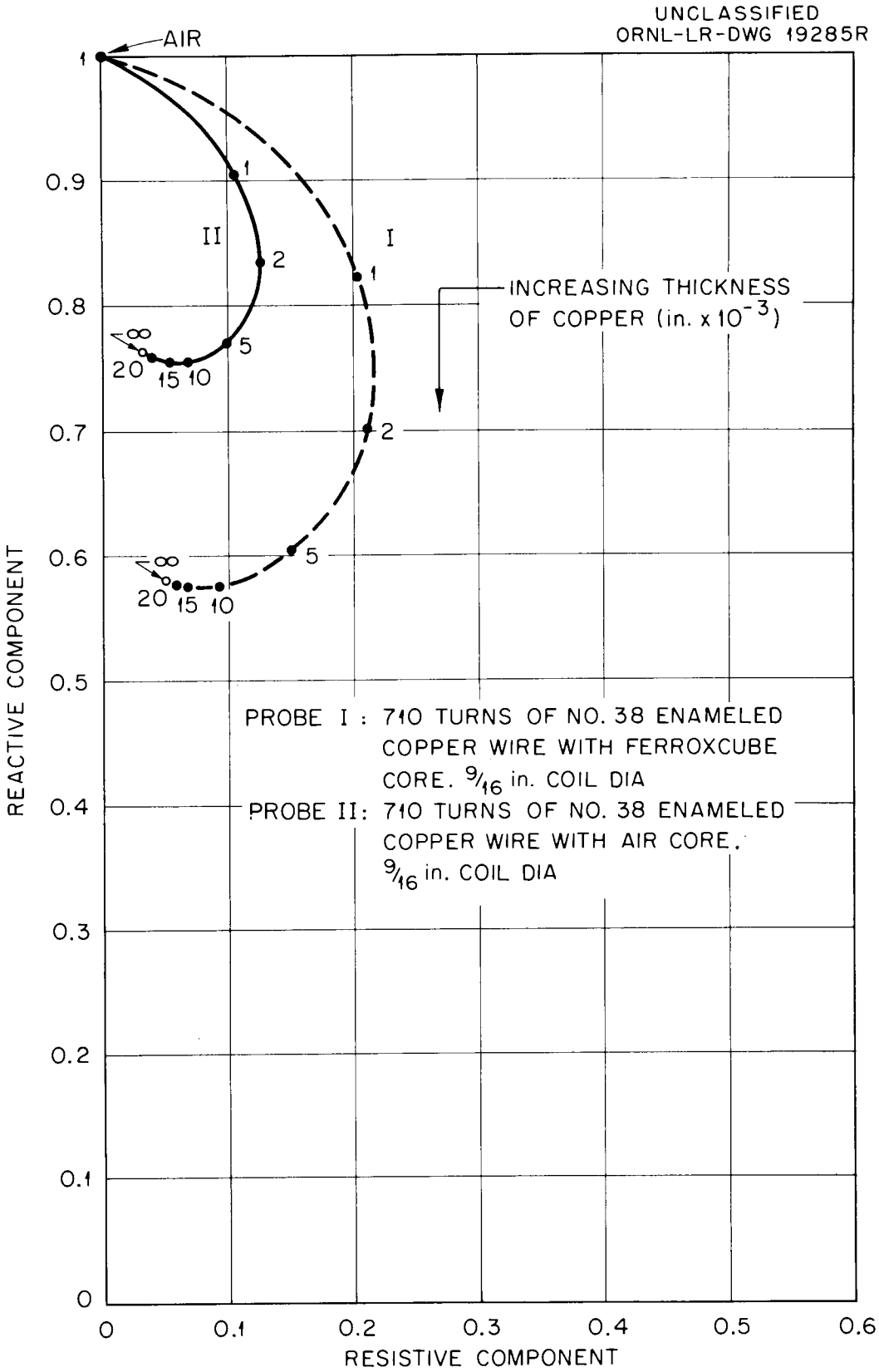

Fig. 13. Comparison of Normalized Impedance Plots of Two Probe Coils at 20 kc as a Function of Copper Thickness.

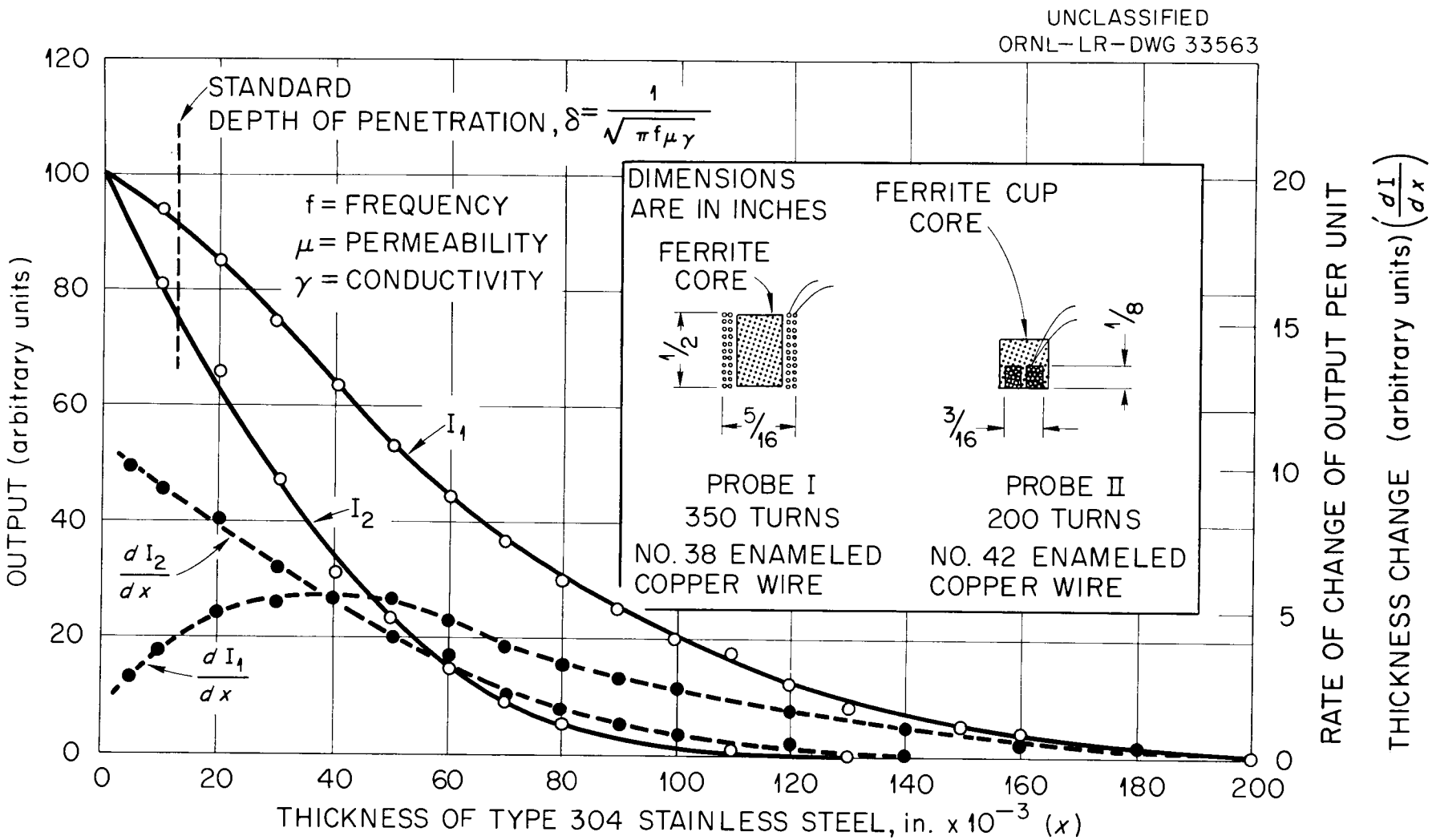

Fig. 14. Sensitivity of Eddy-Current Probe Coils to Thickness Variations at 16 kc.

$$\delta = \frac{1}{\sqrt{\pi f \mu \gamma}}$$

in which

δ = standard depth of penetration,

f = frequency,

μ = permeability, and

γ = conductivity.

This assumes a plane wave impinging upon a semi-infinite conductor. Since these conditions can never be met in practice and since this formula does not contain any terms related to the design of the coil, the standard depth of penetration formula is of little practical use. If this formula held true the response curves for both coils shown would coincide and the depth of penetration would be the same. For purposes of comparison, the standard depth of penetration has been calculated as 0.0133 in. for these test conditions and is marked on the graph.

Also shown in Fig. 14 is the relative sensitivity of each probe to a unit change in thickness. The relative sensitivity (dI_1/dx) of Probe 1 increases with depth until a maximum sensitivity is attained at an approximate total thickness of 0.050 in. and then decreases. Probe 2, however, approaches a maximum sensitivity (dI_2/dx) as the total thickness approaches zero. Thus, it can be seen readily that the probe design is an important consideration when determining testing parameters.

CONCLUSION

Although many successful eddy-current probe-coil techniques have been developed, there is very little information available concerning the design of probe coils and the choice of other testing parameters. Theoretical studies facilitate the understanding of these techniques but provide very little detailed information, since many of the assumptions made to facilitate the mathematical manipulations are not valid in practice. Therefore, the use of empirical methods is necessitated to determine the optimum testing parameters for specific applications. Much additional information from empirical investigations is needed to facilitate the choice of testing parameters for future application.

The application of eddy-current probe-coil techniques to the measurement of thin metal sections and cladding thickness fills a definite need for a measuring method which requires access to only one side of the specimen. Eddy-current techniques have a great advantage in that they are most accurate in the measurement of thin sections which are below the resolving range of resonance ultrasonics. Also, there are very few instances in which cladding-thickness measurements can be successfully accomplished except with eddy-current techniques.

ORNL-2672
Metallurgy and Ceramics
TID-4500 (14th ed.)

INTERNAL DISTRIBUTION

1. C. E. Center
2. Biology Library
3. Health Physics Library
4. Metallurgy Library
5-6. Central Research Library
7. Reactor Experimental Engineering Library
8-27. Laboratory Records Department
28. Laboratory Records ORNL, R.C.
29. A. M. Weinberg
30. L. B. Emlet (K-25)
31. J. P. Murray (Y-12)
32. J. A. Swartout
33. E. H. Taylor
34. E. D. Shipley
35. M. L. Nelson
36. W. H. Jordan
37. C. P. Keim
38. R. S. Livingston
39. R. R. Dickison
40. S. C. Lind
41. F. L. Culler
42. A. H. Snell
43. A. Hollaender
44. M. T. Kelley
45. K. Z. Morgan
46. J. A. Lane
47. A. S. Householder
48. C. S. Harrill
49. C. E. Winters
50. D. S. Billington
51. H. E. Seagren
52. D. Phillips
53. A. J. Miller
54. R. A. Charpie
55. C. F. Leitten
56. E. G. Bohlmann
57. M. J. Skinner
58. P. M. Reyling
59. J. C. Wilson
60. C. O. Smith
61. J. H. Frye, Jr.
62. W. D. Manly
63. J. E. Cunningham
64. G. M. Adamson, Jr.
65-70. J. W. Allen
71. R. J. Beaver
72. E. S. Bomar, Jr.
73. R. E. Clausing
74. J. H. Coobs
75. J. H. DeVan
76. L. M. Doney
77. D. A. Douglas, Jr.
78. E. A. Franco-Ferreira
79. R. J. Gray
80. J. P. Hammond
81. R. L. Heestand
82. T. Hikido
83-117. M. R. Hill
118. E. E. Hoffman
119. H. Inouye
120. L. K. Jetter
121. C. J. McHargue
122. P. Patriarca
123. M. L. Picklesimer
124. T. K. Roche
125. L. D. Schaffer
126. G. P. Smith, Jr.
127. A. Taboada
128. W. C. Thurber
129. R. C. Waugh
130. H. L. Yakel, Jr.
131-136. R. A. Nance
137. J. H. Koenig (consultant)
138. H. Leidheiser, Jr. (consultant)
139. Cyril S. Smith (consultant)
140. H. A. Wilhelm (consultant)
141. ORNL - Y-12 Technical Library, Document Reference Section

EXTERNAL DISTRIBUTION

142. Division of Research and Development, AEC-ORO
143-628. Given distribution as shown in TID-4500 (14th ed.,) under Metallurgy and Ceramics.